Title

Electroconductive agarose hydrogels modulate mesenchymal stromal cell adhesion and spreading through protein adsorption

Journal

Journal of Biomedical Materials Research Part A, 111(5)

ISSN

1549-3296

Authors

Casella, Alena

Panitch, Alyssa

Leach, J Kent

Publication Date

2023-05-01

DOI

10.1002/jbm.a.37503

Peer reviewed

HHS Public Access

Author manuscript

J Biomed Mater Res A. Author manuscript; available in PMC 2024 May 01.

Published in final edited form as:

J Biomed Mater Res A. 2023 May ; 111(5): 596–608. doi:10.1002/jbm.a.37503.

Electroconductive agarose hydrogels modulate MSC adhesion and spreading through protein adsorption

Alena Casella[1,2], **Alyssa Panitch**[3,4,#], **J. Kent Leach**[1,2,#]

[1]Department of Biomedical Engineering, University of California Davis, Davis, CA 95616

[2]Department of Orthopaedic Surgery, School of Medicine, UC Davis Health, Sacramento, CA 95817

[3]Department of Biomedical Engineering, Georgia Institute of Technology, Atlanta, GA 30332

[4]Department of Biomedical Engineering, Emory University, Atlanta, GA 30322

Abstract

Electrically conductive biomaterials direct cell behavior by capitalizing on the effect of bioelectricity in tissue homeostasis and healing. Many studies have leveraged conductive biomaterials to influence cells and improve tissue healing, even in the absence of external stimulation. However, most studies using electroactive materials neglect characterizing how the inclusion of conductive additives affects the material's mechanical properties, and the interplay between substrate electrical and mechanical properties on cell behavior is poorly understood. Furthermore, mechanisms dictating how electrically conductive materials affect cell behavior in the absence of external stimulation are not explicit. In this study, we developed a mechanically and electrically tunable conductive hydrogel using agarose and the conductive polymer PEDOT:PSS. Under certain conditions, we observed that the hydrogel physical and electrical properties were decoupled. We then seeded human mesenchymal stromal cells (MSCs) onto the hydrogels and observed enhanced adhesion and spreading of MSCs on conductive substrates, regardless of the hydrogel mechanical properties, and despite the gels having no cell-binding sites. To explain this observation, we measured protein interaction with the gels and found that charged proteins adsorbed significantly more to conductive hydrogels. These data demonstrate that conductivity promotes cell adhesion, likely by facilitating increased adsorption of proteins associated with cell binding, providing a better understanding of the mechanism of action of electrically conductive materials.

Keywords

conductive hydrogel; mesenchymal stromal cells; electroactive biomaterial; PEDOT:PSS; protein adsorption

Corresponding author: J. Kent Leach, Ph.D., University of California, Davis, Department of Orthopaedic Surgery, 4860 Y Street, Suite 3800, Sacramento, CA 95817, jkleach@ucdavis.edu, (916) 734-8965.
[#]contributed equally as co-senior authors

Disclosure statement
The authors have nothing to disclose.

1. Introduction

Bioelectricity is involved in tissue homeostasis and plays a critical role in developmental processes such as embryonic development and tissue regeneration. Bioelectricity directs cell migration, adhesion, and proliferation[1,2] and aids in the maturation of electroactive cell types. For example, bioelectric signaling promotes neuronal cell differentiation and synchronous beating of cardiomyocytes[3,4]. Unlike other biophysical properties of hydrogels such as stiffness and viscoelasticity, the potential of electrical cues to influence cell behavior is less investigated. Electrically conductive (EC) materials can promote nerve[5,6], cardiac[7,8], muscle[9,10], and bone[11,12] regeneration, and numerous reports indicate that conductive materials can alter cell behavior towards desired outcomes even in the absence of external electrical stimulation[13,14]. However, the mechanism of how conductive materials promote these outcomes is not well understood, thereby limiting our capacity to design new materials for tissue regeneration[15].

Many studies investigating EC hydrogels report both electrical and mechanical characterization of their materials, while some demonstrate synergistic effects between physical and electrical cues on cell behavior[16,17]. However, few report whether they can be decoupled and how their interplay affects cell behavior. Thus, there is a significant need to develop an effective model system to interrogate these basic relationships. There is a substantial body of evidence that demonstrates the importance of directing cell behavior *via* biophysical properties[18-20] that may be tuned using multiple approaches (*e.g.*, increasing polymer concentration, varying crosslinker type or strength, modulating adhesivity[14,20,21]). For electrically conductive hydrogels, the conductive properties are commonly tuned by doping with electrically or ionically[13] conductive additives such as carbon- or metal-based materials and synthetic polymers with conjugated bond structures. These materials all face drawbacks of being nondegradable[22,23] and are poorly soluble, making them difficult to incorporate into hydrogels without further modification[24]. PEDOT:PSS is commonly added to hydrogel biomaterials owing to its commercial availability, water-dispersibility, and non-cytotoxicity[25,26].

Here, we used poly(3,4-ethylenedioxythiophene) polystyrene sulfonate (PEDOT:PSS) to manipulate the conductivity of hydrogels and interrogate the interplay of substrate stiffness and conductivity on cell behavior. We developed a mechanically and electrically tunable hydrogel system using widely available materials and methods that are accessible for most research groups. We interrogated the contribution of protein adsorption to these hydrogels as a potential mechanism of action. We then investigated human MSC response to physical and electrical cues and hypothesized that cells cultured on conductive hydrogels would have increased cell adhesion regardless of biophysical properties.

2. Materials and Methods

2.1 Fabrication of PEDOT:PSS agarose hydrogels

Agarose (Thermo Fisher Scientific, Waltham, MA) was dissolved in ultrapure water to 2.5 wt% and mixed with PEDOT:PSS (PH1000, Ossila, Sheffield, UK) and water in various ratios to make hydrogels with final concentrations of 0.5 or 1.0 wt% agarose and 0.0, 0.2

or 0.6 wt% PEDOT:PSS (Table 1). PEDOT:PSS was sonicated for 15 min prior to hydrogel fabrication, and water was warmed to extend gelation time, allowing for adequate mixing. Hydrogel pre-polymer was deposited into glass-mounted PDMS molds (1.5 mm thick x 8 mm I.D.) and allowed to set at room temperature for at least 10 min to make 80 μL gels. After complete gelation, hydrogels were transferred to 24 well plates containing 1 mL of either αMEM (Invitrogen, Waltham, MA) supplemented with 10% FBS (GenClone, San Diego, CA) and 1% penicillin-streptomycin (Gemini Bio Products) or ultrapure water to remove any unreacted reagents. Gels stored in αMEM were maintained in standard cell culture conditions (*i.e.*, 37°C, 5% CO_2), whereas gels stored in water were kept at room temperature. Pure PEDOT:PSS gels were fabricated by mixing PEDOT:PSS and 4-dodecylbenzenesulfonic acid (Sigma, St. Louis, MO) at 3 v/v% according to Zhang et al.[27] and used as controls for some biochemical assays (Fig. S1A).

2.2 Characterization of PEDOT:PSS elution and hydrogel degradation

Fifty μL samples of the solution used to store hydrogels (αMEM or ultrapure water) were removed daily in triplicate into clear, flat 96-well plates. Absorbance was measured at 550 nm. The remaining storage solution was aspirated and replaced with fresh solution.

At 1, 3, 7, and 10d, hydrogel wet mass was measured using a standard lab scale after blotting away excess fluid. Gels were then frozen and lyophilized for at least 24 h or until dry. The dry mass of hydrogels was measured with a Mettler Toledo XPR2 Microbalance (Mettler Toledo, Columbus, OH). Swelling ratio (Q) was calculated using Equation 1, as described previously[28].

$$Q = \frac{\left(\frac{W_{Swollen} - W_{Dry}}{\rho_{Water}}\right) + \frac{W_{Dry}}{\rho_{Polymer}}}{\frac{W_{Dry}}{\rho_{Polymer}}} \quad \text{Equation 1:}$$

where ρ is density and ρ_{Water} is 1 g/mL and $\rho_{Polymer}$ is 1.64 g/mL for agarose[29,30].

2.3 Mechanical characterization of hydrogels

At 1, 3, 7 and 10d, we measured the gel shear storage modulus using a Discovery HR2 Hybrid Rheometer (TA Instruments, New Castle, DE) with a stainless steel, cross-hatched, 8-mm plate geometry. After pre-loading each gel with approximately 0.03-0.04 N of axial force in compression, an oscillatory strain sweep ranging from 0.004% to 4% strain was applied to each gel to obtain a linear viscoelastic region (LVR)[31]. At least 5 data points were collected for each LVR and averaged to obtain shear storage modulus.

2.4 Scanning electron microscopy of hydrogels

Eighty μL hydrogels were prepared as described above and immediately transferred to a 35% ethanol solution to initiate critical point drying. Gels were stored in increasing concentrations of ethanol (35%, 50% 75%, 100%) for 15 min each. Then gels were stored in a 1:1 solution of hexamethyldisilazane (HMDS, Sigma) and 100% ethanol and stored for 1 h. Finally, pure HMDS was added to the gels for 5 min. To complete the dehydration process, HMDS was removed, and gels were allowed to air dry for at least 1 h. Gels were

then mounted to aluminum stubs with double-sided carbon tape. Prior to imaging, samples were sputter coated with gold/palladium. Micrographs were taken using a Thermo Fisher Quattro S Environmental SEM.

2.5 Qualitative evaluation of hydrogel hydrophobicity

The hydrophobic or hydrophilic properties of 80 μL gels were assessed qualitatively using solvents with varying surface tension and polarity. One drop of ultrapure water (γ = 72.8 dyn/cm), glycerol (γ = 64.0 dyn/cm; USB Corp., Cleveland, OH), hexane (γ = 18.4 dyn/cm; EMD), or cottonseed oil (γ = 14.9 dyn/cm[32]; Sigma) was applied to the surface of a hydrogel, and an image of the beading or spreading of the drop was captured using a Nikon D3300 DSLR camera with an APO 180 mm F2.8 EX macro lens (Sigma Corporation, Japan).

2.6 Electrical characterization of hydrogels

The electrical properties of hydrogels were measured using a custom two-point setup depicted in Figure 3A. Hydrogels were constrained by a PDMS mold (I.D. 10 mm, thickness 1.5 mm) and sandwiched between two brass plates. The sandwich was stabilized between the jaws of a tabletop angle vise. One brass plate was connected to a power supply (BK Precision 1735A, Yorba Linda, CA) using alligator clips, and the other brass plate was connected to a multimeter (SparkFun Electronics, Niwot, CO) to measure current. Voltages ranging from 100 to 500 mV, a range selected to avoid electrolysis of water, were applied to the gels to obtain current-voltage curves. After testing, hydrogel thickness and diameter were measured with calipers. Current-voltage curves were analyzed for linearity, and datasets with an R^2 value of ≥0.9 were accepted for resistance calculations. Conductivity was calculated using Pouillet's law (Equation 2).

$$\sigma = \frac{t}{RA} \quad \text{Equation 2:}$$

where σ is conductivity in S/cm, t is thickness of the hydrogel (cm), R is resistance (Ω), and A is cross-sectional area (cm^2). Hydrogels for conductivity testing were stored in ultrapure water to eliminate the confounding effects of ions in PBS and αMEM.

2.7 Adsorption of fibronectin to acellular gels

Acellular gels for protein adsorption studies were stored in 1X PBS. After aspirating the storage solution, 1 mL of a 40 μg/mL fibronectin solution in PBS (FN, EMD Millipore, Burlington, MA) was added and allowed to incubate at 37°C for 24 h. FN was added to wells without gels to calculate protein adsorption to the plate. After incubation, the solution in each well was collected and analyzed for protein content using the Micro bicinchoninic acid (MicroBCA) Protein Assay Kit (Thermo Fisher Scientific). To characterize the kinetics of FN adsorption, this experiment was repeated with incubation times of 10 s and 30 min.

Protein concentration was calculated using the Assayfit Pro online software (https://www.assayfit.com) with a 2° polynomial curve fit. Concentrations were multiplied by an absorbance ratio to account for protein-to-protein variation, since BSA was used for the

standard curve. The absorbance ratio was calculated by dividing the concentration of protein reported by the assay by the known concentration of protein (Equation 3).

$$Absorbance\ Ratio = \frac{C_{Assay}}{C_{Known}} \quad \text{Equation 3:}$$

The concentration of FN adsorbed to the gels (C_{Gel}) was calculated by subtracting the concentration of FN adsorbed to the plate (C_{Plate}) and the concentration of FN in solution (C_{Sol}) from the concentration of protein initially delivered to each gel (C_{Tot}), as shown in Equation 4. The percent of FN solution retained by the gel was calculated by dividing C_{Gel} by C_{Tot} and multiplying by 100.

$$C_{Gel} = C_{Tot} - (C_{Plate} + C_{Sol}) \quad \text{Equation 4:}$$

2.8 Adsorption of charged proteins to acellular gels

To study the influence of conductive polymer on protein adsorption more broadly, gel formulations (100 μL from Table 1) were pipetted into 96-well plates and stored in ultrapure water. After aspirating the storage water, 200 μL of protein solution were pipetted on top of gels and allowed to incubate for 24 h. Charged protein solutions were PBS containing 1 mg/mL of BSA (Gemini Bio Products, Sacramento, CA), which takes on a negative charge in neutral solution; lysozyme from chicken egg (EMD) which takes on a positive charge in neutral solution; or myoglobin from equine heart (EMD), which is neutral in neutral solution. After 24 h, the protein solutions were analyzed using a BCA Protein Assay Kit (Thermo Fisher Scientific) and analyzed as described above, but with a four-parameter logistic curve fit, per the manufacturer's instructions.

2.9 Cell culture

Human MSCs (RoosterBio, Frederick, MD) were cultured in complete media (αMEM, 10% FBS, 1% P/S) in standard culture conditions. MSCs were used at passage 4-6 for all experiments.

Eighty μL gels were fabricated as described above and stored in sterile ultrapure water in a cell culture incubator. Prior to cell seeding, storage water was changed three times, with approximately 4 h between changes, to allow for PEDOT:PSS elution. MSCs were trypsinized, pelleted, and resuspended with fresh media at 5 x 10^5 cells/mL. After aspirating the storage water from the gels, 10 μL of cell suspension were pipetted onto one side of the gel followed by a 10 min incubation in standard culture conditions. Next, gels were flipped and 10 μL of the same cell suspension were added to the other side of the gel. After 10 min, 1 mL of αMEM was added to each well. Media was changed every 2-3 days, and gels were analyzed after 1, 3, and 7d.

2.10 Assessment of viability, proliferation, and metabolic activity

Metabolic activity from the cells was measured with the alamarBlue assay (Thermo Fisher Scientific) according to the manufacturer's instructions. Results were normalized

to DNA content measured using the Quant-iT PicoGreen dsDNA Assay Kit (Thermo Fisher Scientific). Viability of the cells on gels was determined using a LIVE/DEAD stain where viable cells were stained green with calcein AM (Invitrogen) and dead cells were stained red with propidium iodide (Millipore Sigma, St. Louis, MO). Cell adhesion and spreading was visualized by fixing the gels in 4% paraformaldehyde and staining the cells with Alexa Fluor 488 Phalloidin and DAPI (both from Invitrogen). Cells on gels were imaged using a Nikon Eclipse T32000U microscope.

2.11 Statistical analysis

Data are presented as means ± standard deviation. Statistical analysis was performed using GraphPad Prism 9 software using t-tests and one-way or multi-way analysis of variance with Tukey correction for multiple comparison. A mixed-effects analysis model was used for datasets with unequal group sizes. Differences were considered statistically significant at $p \leq 0.05$. Groups that are significantly different are denoted with different letters, while groups that share letters are statistically similar.

3. Results

3.1 PEDOT:PSS-laden agarose hydrogels maintain their structure over time

Mechanical properties of hydrogels were tuned using two different concentrations of agarose (0.5 or 1.0 wt%), while electrical properties were tuned *via* concentration of PEDOT:PSS (0.0, 0.2, or 0.6 wt%). All hydrogels remained intact for the course of the study (Fig. 1A). The incorporation of higher concentrations of PEDOT:PSS, a blue-black polymer, resulted in hydrogels becoming increasingly dark and opaque. While each gel was formulated such that respective groups contained either the same amount of agarose or PEDOT:PSS, the color difference between 0.5 and 1.0 wt% agarose gels containing PEDOT:PSS (both 0.2 and 0.6 wt%) indicates that less EC polymer was incorporated. This may be due to fewer polymeric entanglements or PSS-agarose crosslinks formed in gels containing less polysaccharide.

After formation, gels were stored in αMEM or ultrapure water to wash away any unincorporated reagents, and storage solution was replaced daily. Storage αMEM did not grossly appear to change color over time (Fig. 1B). Absorbance values fluctuated only slightly and did not appreciably deviate from baseline (Fig. 1C). These data suggest minimal PEDOT:PSS leaching from the gels in this environment. Swelling ratio decreased over time for groups containing PEDOT:PSS (Fig. 1D). With daily replenishment of αMEM, we predict that charged moieties from the cell culture media (*e.g.*, salts and proteins) accumulate within the hydrogel, causing an increase in dry mass over time, which we report in Fig. S2.

Observations of PEDOT:PSS elution in water contrast strikingly to gels stored in αMEM. Storage water was noticeably gray after 24 h (Fig. S3A) and absorbance values of the water decreased significantly between 1 and 2 d, indicating PEDOT:PSS elution from the gels. After the initial time point, absorbance values were near zero and gels appeared to reach an equilibrium with the storage water (Fig. S3B). The dry mass of hydrogels containing

PEDOT:PSS also exhibited a decline after 1d, though this may be attributed to the loss of PEDOT:PSS (Fig. S3C). Hydrogel swelling ratio increased after fabrication but equilibrated after 1d (Fig. S3D). The 0.5 wt% agarose gels had significantly higher swelling ratios at each time point, regardless of PEDOT:PSS concentration (Fig. S3E), which may also be attributed to the reduced polymeric entanglements compared to the 1.0 wt% agarose gels.

These data establish the degradation and dissociation properties of the hydrogels used for the remaining studies. Furthermore, these findings illustrate the capacity of conductive additives to elute out of hydrogel materials, emphasizing the importance of material storage prior to characterization.

3.2 Mechanical and electrical properties of agarose hydrogels can be decoupled

Hydrogel storage modulus was predominantly influenced by wt% agarose when gels were stored in αMEM, though increases ($p \leq 0.05$) were observed in the 0.5 wt% agarose gels when 0.6 wt% PEDOT:PSS was added (Fig. 2A). To confirm the driving factor was wt% agarose, we analyzed the storage moduli for all hydrogels at each agarose concentration, regardless of PEDOT:PSS loading. There was a significant increase in storage modulus from approximately 1.75 kPa to 9.5 kPa with increasing agarose content ($p \leq 0.0001$) (Fig. 2B). While 0.6 wt% PEDOT:PSS caused a significant increase in storage modulus in the 0.5 wt% agarose gels ($p \leq 0.0001$) (Fig. 2C), the magnitude of this difference was less than the magnitude of the difference in storage modulus between the 0.5 and 1.0 wt% agarose gels (Fig. 2B). By contrast, when storage modulus was analyzed as a function of PEDOT:PSS content for the 1.0 wt% agarose gels, PEDOT:PSS did not cause a change in mechanical properties (Fig. 2D). Pure PEDOT:PSS gels had statistically similar mechanical properties to the 0.5 wt% agarose gels, with an average storage modulus of approximately 2.6 kPa (Fig. S3C).

Gels stored in ultrapure water exhibited similar relationships but were more susceptible to changes with the addition of 0.2 wt% PEDOT:PSS (Fig. S4A, $p \leq 0.05$). This may be due to more pronounced dissociation over time when gels were stored in water (Fig. S3). Although both 0.5 and 1.0 wt% agarose gels had higher storage moduli with the addition of PEDOT:PSS, the magnitude of change in storage modulus as a function of wt% agarose (Fig. S4B, $p \leq 0.0001$) was greater than as a function of wt% PEDOT:PSS (Fig. S4C,D; $p \leq 0.0001$). These data further highlight the importance of storage conditions on material characterization. Taken together, analysis of storage modulus indicates that below a certain concentration, the addition of PEDOT:PSS does not affect hydrogel biophysical properties. Thus, these data fulfill half of the requirements towards our aim of developing a hydrogel system that is electrically and mechanically decoupled.

As expected, electrical conductivity of PEDOT:PSS agarose hydrogels was predominantly driven by PEDOT:PSS content (Fig. 3B). When conductivity was analyzed as a function of agarose concentration, conductivity increased 1.2-fold with increased agarose concentration ($p \leq 0.05$) (Fig. 3C). Conductivity measurements of hydrogels formed from each agarose concentration (without PEDOT:PSS) confirmed that agarose has some intrinsic conductivity (Fig. 3B), which may contribute to trends of increased conductivity between 0.5 and 1.0 wt% agarose gels for all concentrations of PEDOT:PSS. However, when analyzing

conductivity as a function of wt% PEDOT:PSS only, we observed nearly a 2-fold increase in conductivity when increasing PEDOT:PSS concentration from 0 to 0.2 wt% ($p \leq 0.0001$) (Fig. 3D). Interestingly, we did not detect significant increases in conductivity when PEDOT:PSS concentration was further increased. Conductivities ranged from approximately 2×10^{-6} to 8×10^{-6} S/cm, classifying these materials as semiconductors and appropriate for biological applications. At approximately 3×10^{-2} S/cm, pure PEDOT:PSS hydrogels had 4 orders of magnitude higher conductivity than the agarose-based gels (Fig. S1D).

These data provide evidence that the physical and electrical properties of this hydrogel model system can be decoupled. For example, while storage modulus did not change for 1.0 wt% agarose gels doped with 0.0 or 0.2 wt% PEDOT:PSS (Fig. S4), there was a difference in conductivity between these groups (Fig. 3C). While not all groups within this hydrogel platform had decoupled electrical and mechanical properties, we studied cell response to all hydrogel conditions. This strategy allowed us to interrogate if cells respond differently to substrates with and without decoupled properties. Additionally, since no differences in storage modulus or conductivity were observed between the gels on 7 and 10d (*data not shown*), the subsequent *in vitro* studies were carried out only to 7d.

3.3 Conductive hydrogels support cell viability and metabolic activity at early timepoints

MSCs cultured on 0.5 and 1.0 wt% agarose exhibited greater viability at 7d when gels were conductive (Fig. 4A,D). LIVE/DEAD imaging revealed the most cell adhesion to substrates containing PEDOT:PSS with little adhesion to non-conductive controls. Minimal cell adhesion was observed at 1d, and cell viability *via* the LIVE/DEAD assay appeared to peak on 3d (Fig. S5). Of the cells that adhered, most were viable, indicated by calcein AM staining. Pure PEDOT:PSS supported cell viability through 7d, but cells appeared most viable at 3d (Fig. S1E).

Metabolic activity *via* alamarBlue was higher for cells cultured on conductive substrates, and raising the concentration of PEDOT:PSS further increased cell activity at 1 and 3d (Fig. 4B,E). DNA content was nearly constant for all 0.5 wt% agarose groups at each timepoint, but DNA mass was greatest at 3d ($p \leq 0.0001$), indicating cell proliferation (Fig. 4C). A similar relationship was observed in the DNA content of cells cultured on 1.0 wt% agarose gels, though conductivity promoted cell proliferation at 3 and 7d over non-conductive controls (Fig. 4F). While cell metabolic activity decreased over time, conductivity boosted cell behavior compared to the non-conductive controls, which had nearly no cell activity, even at 1d. Pure PEDOT:PSS gels did not consistently promote MSC metabolic activity (Fig. S1F).

3.4 Conductive hydrogels support cell adhesion and spreading

MSCs cultured on gels containing 1.0 wt% agarose were fixed and stained with DAPI and phalloidin to visualize adhesion and spreading (Fig. 5A). While some cells adhered to the non-conductive controls, their morphology was rounded. Furthermore, irregular staining on these gels at 7d is indicative of debris. This contrasts strikingly with the cells on gels containing 0.6 wt% PEDOT:PSS, which exhibit cytoskeletal projections and, by 7d, take on the fibroblastic morphology of healthy MSCs. Pure PEDOT:PSS gels were not effective

at retaining cells or facilitating spreading (Fig. S1G). While adhesion to all gels was low overall, the addition of PEDOT:PSS allowed cells to form strong enough bonds to spread, even in the absence of adhesion ligands and external stimulation.

To elucidate possible mechanisms of this observation, we measured the amount of fibronectin (FN) adsorbed to gels as a function of agarose concentration, PEDOT:PSS concentration, and time. We observed more FN in gels with higher PEDOT:PSS concentration ($p \leq 0.05$) starting as early as 30 min, though this may have been due to FN diffusion into the bulk gel. After 24 h of equilibration, FN content was still greater in PEDOT:PSS-containing groups, which we attributed to a combination of diffusion and adsorption (Fig. 5B,C). This trend was also observed in pure PEDOT:PSS gels (Fig. S1H). The increase in protein adsorption between gels containing 0.2 and 0.6 wt% PEDOT:PSS required further investigation, as there were no significant differences in conductivity between these groups (Fig. 3D). As such, we performed scanning electron microscopy on dehydrated gels. Hydrogels with 0.0 and 0.2 wt% PEDOT:PSS had clear fibrillar and network-like structures, whereas the 0.6 wt% PEDOT:PSS groups had more globular structures, leading to increased surface roughness (Fig. 5D). Surface roughness contributes to protein adsorption, in part by increasing the available surface area. Thus, the 0.6 wt% PEDOT:PSS gels may facilitate more FN interaction due to their topography[32]. We also qualitatively investigated the hydrophobic properties of the hydrogels. We did not observe striking differences in hydrophobicity with presence of PEDOT:PSS, with the exception of the 0.5 wt% agarose gels, where the edges of the water drop are visible on the gels containing PEDOT:PSS (Fig. S6).

3.5 Conductive hydrogels promote adsorption of charged proteins

To further understand how conductive hydrogels facilitated fibronectin adsorption and cell adhesion in the absence of cell-binding ligands, we examined whether conductivity promoted electrostatically driven protein adsorption. To that aim, we dissolved proteins with varying isoelectric points in PBS, where they took on net charge (BSA (−), lysozyme (+), and myoglobin (neutral)) (Fig. 6A) and added them to acellular hydrogels. The adsorption of charged proteins (BSA and lysozyme) correlated with PEDOT:PSS concentrations for both 0.5 and 1.0 wt% agarose gels (Fig. 6B,C). Myoglobin was unaffected by conductivity or storage modulus (*i.e.*, wt% agarose). Interestingly, for the 0.5 wt% agarose gels, there was a greater level of significance in adsorption between the non-conductive and 0.6 wt% PEDOT:PSS groups. By contrast, in the 1.0 wt% agarose gels, the increase in protein adsorption was more significant between the non-conductive and 0.2 wt% PEDOT:PSS gels, with less of an increase between the 0.2 and 0.6 wt% PEDOT:PSS groups. This may be attributed to reduced retention of PEDOT:PSS by the 0.5 wt% agarose gels.

These data indicate that conductive substrates have increased surface charges that electrostatically interact with other charged molecules. Increased cell adhesion to conductive substrates is likely driven by the adsorption of charged proteins in the cell culture media that facilitate adhesion (*e.g.*, albumin). These findings align with our observation of increased FN adsorption, which takes on a moderately negative charge in PBS and is known to enable cell adhesion.

4. Discussion

Electrically conductive biomaterials are a promising tool to influence cell behavior given their ability to facilitate bioelectric signaling, which is frequently linked to tissue development and wound healing. While using conductive materials to imbue hydrogels with electroactive properties is becoming more commonplace, few studies investigate how changing the electrical characteristics of a material affect its other properties. Beyond that, the interplay of electrical and physical properties and how they affect cell behavior is understudied.

In this work, we used agarose and PEDOT:PSS to create an electrically and mechanically tunable hydrogel platform. PEDOT:PSS is frequently used for creating conductive biomaterials and boasts the advantage of being water-dispersible compared to other synthetic polymers which are strongly hydrophobic. Numerous hydrogels and polymers are suitable to make mechanically tunable biomaterials for tissue engineering. Agarose is among the easiest to fabricate, and mechanical tunability is controlled simply by changing the concentration of polysaccharide, thereby reducing variability between samples. While agarose is inherently non-adhesive, cell-binding moieties can be added by incorporating collagen or chemically modifying the agarose backbone to make it amenable to covalent bonding of adhesive peptides[33,34]. This contrasts with other commonly used biomaterials such as collagen, alginate, or GelMA, which have additional variables beyond polymer concentration that affect mechanical properties. Interpenetrating networks[35] and electrospun scaffolds[36] have been formed into conductive substrates but require more complex protocols to fabricate.

With this platform, we interrogated fundamental cell behaviors such as viability, adhesion, and metabolic activity. We observed significant differences in protein adsorption and cell adhesion on conductive substrates. Without the inclusion of adhesive ligands, we did not expect this material to effectively promote cell behavior. However, given significant differences between the PEDOT:PSS-containing groups and agarose-only controls, this work still illustrates the influence of EC moieties in hydrogels, even in the absence of external stimulation. Future work will incorporate conductive additives into other hydrogel materials with different tunable mechanical properties (*e.g.*, adhesive ligand concentration, stress-relaxation, etc.) to further probe the relationships between biophysical and electrical properties. Additionally, while synthetic conductive polymers and carbon-based materials are frequently used in biomaterials, emerging studies using naturally derived[37] and ionically conductive[3,13] additives show strong promise for making bioresorbable and clinically translatable biomaterials.

The stiffness and storage moduli of conductive hydrogels vary greatly depending on the application. The storage moduli of our hydrogels ranged from approximately 2-12 kPa, suitable for mimicking the mechanical properties of a variety of soft tissues (*e.g.*, nerve and muscle)[18]. Similar storage moduli have been reported in studies using collagen-based-[38] and fibrin-alginate gels[39]. While storage moduli of our gels was primarily influenced by the concentration of agarose, the addition of PEDOT:PSS also affected their biophysical properties. For the 0.5 wt% agarose gels, addition of 0.6 wt% PEDOT:PSS caused a

significant increase in storage modulus, though the magnitude of this increase was less than that observed by increasing the agarose concentration. By contrast, the storage modulus of the 1.0 wt% agarose gels was unaffected by PEDOT:PSS. Other studies have also reported changes in mechanical properties with addition of conductive polymers. Song et al. observed increased Young's modulus and hardness when adding polypyrrole to reduced graphene oxide scaffolds[40]. The addition of polypyrrole to alginate hydrogels also yielded significantly higher Young's moduli in proportion to polypyrrole concentration[41]. These data demonstrate the importance of testing the influence of conductive additives on material biophysical properties.

The conductive properties of the materials used in this study matched the properties of other electrically conductive hydrogels [11]. Conductivities for EC hydrogels range from approximately 10^{-6} S/cm for carbon nanotubes incorporated into silk fibroin[42] to 10^{-2} S/cm for PEDOT-hyaluronic acid nanoparticles mixed into a chitosan hydrogel[43]. Most gels fall within the range of 10^{-6}-10^{-3} S/cm, on par with the conductivities of endogenous tissues (10^{-5}-10^{-3} S/cm)[15]. For example, Basurto and colleagues made polypyrrole-containing scaffolds on the order of 10^{-5} S/cm and reported increased myogenic maturation when C2C12s were seeded on conductive scaffolds. Interestingly, the benefits of conductivity are not limitless, as continued increases in conductivity can have detrimental effects on cell metabolic activity[10]. Furthermore, a study by Marzocchi and colleagues illustrates changes in proliferation of different cell lines depending on the oxidation state of PEDOT:PSS, highlighting the need to characterize and control material electrical properties for *in vitro* applications[44]. Collectively, these data emphasize the importance of designing materials with electrical properties that match those of native tissues. However, bioelectricity fluctuates throughout regenerative processes and may serve as a new target for material electrical properties[45].

The positive effects of conductive substrates on cell behavior are frequently attributed to the materials' ability to facilitate protein adsorption[46]. In the seminal paper by Schmidt et al., the authors postulate that the negative surface charge of polypyrrole led to increased adsorption of positively charged proteins, which led to subsequent PC-12 adhesion and extension[47]. However, studies that demonstrate surface charge properties of conductive biomaterials are rare. Inspired by prior work[48,49], we used proteins with different isoelectric points to interrogate the surface charge properties of agarose and PEDOT:PSS hydrogels. Adsorption of both positively and negatively charged proteins increased with increasing PEDOT:PSS concentrations, particularly for the gels containing a higher concentration of agarose. While PEDOT:PSS has both positive and negative charges in its chemical structure that may contribute to this phenomenon, charged materials also rearrange the distribution of surface charges to accommodate other charged moieties with which they interact in order to achieve electroneutrality[50]. It is possible that proteins change their conformation as they interact with a conductive substrate, which merits future investigation. However, changes observed in the physical properties of the hydrogels corroborate the role of electroneutrality. With increased electrostatically driven protein adsorption to the gel surface and throughout the bulk construct, we predict charges within the polymer network were progressively shielded. Charge shielding limited charge repulsion within the hydrogel, leading to decreased swelling ratio, despite increases in dry mass. We

also qualitatively assessed the hydrophobic properties of the gels and observed minimal differences between groups, regardless of PEDOT:PSS presence. We anticipate that the PSS^- shell, $PEDOT^+$ core structure of PEDOT:PSS is uninterrupted in the aqueous state of hydrogels, rendering similar behaviors between PEDOT:PSS-containing and undoped agarose gels[27]. It is also possible that, if exposed in a hydrophilic environment, PEDOT will rearrange or phase separate to minimize its exposure to the polar, or more hydrophilic, environment[51]. For this reason, it is not surprising that the hydrogels have minimal change in hydrophobic character. Finally, our conductive gels promoted MSC adhesion and spreading compared to non-conductive control groups. While this may be attributed to increased adsorption of proteins found in the cell culture media, it will be important to investigate cell-binding pathways in response to conductive substrates.

In this work, we illustrate the progression of fabricating an electrically conductive hydrogel system in which mechanics and conductivity can be decoupled, allowing us to study the influence of each on cell behavior. We demonstrate that conductive hydrogels facilitate MSC adhesion and spreading and provide evidence that these improvements in cell behavior may be linked to changes in protein adsorption to conductive hydrogels. These studies fill important knowledge gaps when using electrically conductive materials for biological applications. These findings highlight the importance of thorough material characterization and provide mechanistic insight into how cell behavior is influenced by conductive materials, even when not externally stimulated. Additionally, the methods for incorporating conductive additives and characterizing hydrogel electrical properties are highly accessible for most research groups, providing a means for others to expand into this growing field.

Supplementary Material

Refer to Web version on PubMed Central for supplementary material.

Acknowledgements

Research reported in this publication was supported by National Institute of Dental and Craniofacial Research of the National Institutes of Health under award number R01 AR079211 and R01 DE025899 to JKL. AC was funded by the Floyd and Mary Schwall Fellowship in Medical Research, the UC Davis Dean's Distinguished Graduate Fellowship, and the ARCS Foundation. The content is solely the responsibility of the authors and does not necessarily represent the official views of the National Institutes of Health. The funders had no role in the decision to publish, or preparation of the manuscript. JKL gratefully acknowledges financial support from the Lawrence J. Ellison Endowed Chair of Musculoskeletal Research. Schematics were created with BioRender.com.

REFERENCES

[1]. Levin M, Pezzulo G, Finkelstein JM, Endogenous bioelectric signaling networks: exploiting voltage gradients for control of growth and form, Annu Rev Biomed Eng. 19 (2017) 353–387. 10.1146/annurev-bioeng-071114-040647. [PubMed: 28633567]

[2]. Funk RH, Endogenous electric fields as guiding cue for cell migration, Front Physiol. 6 (2015) 143. 10.3389/fphys.2015.00143. [PubMed: 26029113]

[3]. Walker BW, Lara RP, Yu CH, Sani ES, Kimball W, Joyce S, Annabi N, Engineering a naturally-derived adhesive and conductive cardiopatch, Biomaterials. 207 (2019) 89–101. 10.1016/j.biomaterials.2019.03.015. [PubMed: 30965152]

[4]. Cui Z, Ni NC, Wu J, Du GQ, He S, Yau TM, Weisel RD, Sung HW, Li RK, Polypyrrole-chitosan conductive biomaterial synchronizes cardiomyocyte contraction and improves myocardial

electrical impulse propagation, Theranostics. 8 (2018) 2752–2764. 10.7150/thno.22599. [PubMed: 29774073]

[5]. Zhou L, Fan L, Yi X, Zhou Z, Liu C, Fu R, Dai C, Wang Z, Chen X, Yu P, Chen D, Tan G, Wang Q, Ning C, Soft conducting polymer hydrogels cross-linked and doped by tannic acid for spinal cord injury repair, ACS Nano. 12 (2018) 10957–10967. 10.1021/acsnano.8b04609. [PubMed: 30285411]

[6]. Zhou X, Yang A, Huang Z, Yin G, Pu X, Jin J, Enhancement of neurite adhesion, alignment and elongation on conductive polypyrrole-poly(lactide acid) fibers with cell-derived extracellular matrix, Colloids Surf B Biointerfaces. 149 (2017) 217–225. 10.1016/j.colsurfb.2016.10.014. [PubMed: 27768911]

[7]. Roshanbinfar K, Vogt L, Greber B, Diecke S, Boccaccini AR, Scheibel T, Engel FB, Electroconductive biohybrid hydrogel for enhanced maturation and beating properties of engineered cardiac tissues, Adv. Funct. Mater 28 (2018) 1803951. 10.1002/adfm.201803951.

[8]. Zhang C, Hsieh M-H, Wu S-Y, Li S-H, Wu J, Liu S-M, Wei H-J, Weisel RD, Sung H-W, Li R-K, A self-doping conductive polymer hydrogel that can restore electrical impulse propagation at myocardial infarct to prevent cardiac arrhythmia and preserve ventricular function, Biomaterials. 231 (2020) 119672. 10.1016/j.biomaterials.2019.119672. [PubMed: 31841751]

[9]. Zhang M, Guo B, Electroactive 3D scaffolds based on silk fibroin and water-bornepolyaniline for skeletal muscle tissue engineering, Macromol Biosci. 17 (2017) 1700147. 10.1002/mabi.201700147.

[10]. Basurto IM, Mora MT, Gardner GM, Christ GJ, Caliari SR, Aligned and electrically conductive 3D collagen scaffolds for skeletal muscle tissue engineering, Biomater. Sci 9 (2021) 4040–4053. 10.1039/d1bm00147g. [PubMed: 33899845]

[11]. Guex AG, Puetzer JL, Armgarth A, Littmann E, Stavrinidou E, Giannelis EP, Malliaras GG, Stevens MM, Highly porous scaffolds of PEDOT:PSS for bone tissue engineering, Acta Biomater. 62 (2017) 91–101. 10.1016/j.actbio.2017.08.045. [PubMed: 28865991]

[12]. Chen J, Yu M, Guo B, Ma PX, Yin Z, Conductive nanofibrous composite scaffolds based on in-situ formed polyaniline nanoparticle and polylactide for bone regeneration, J Colloid Interface Sci. 514 (2018) 517–527. 10.1016/j.jcis.2017.12.062. [PubMed: 29289734]

[13]. Noshadi I, Walker BW, Portillo-Lara R, Shirzaei Sani E, Gomes N, Aziziyan MR, Annabi N, Engineering biodegradable and biocompatible bio-ionic liquid conjugated hydrogels with tunable conductivity and mechanical properties, Sci Rep. 7 (2017) 4345. 10.1038/s41598-017-04280-w. [PubMed: 28659629]

[14]. Solazzo M, Krukiewicz K, Zhussupbekova A, Fleischer K, Biggs MJ, Monaghan MG, PEDOT:PSS interfaces stabilised using a PEGylated crosslinker yield improved conductivity and biocompatibility, J Mater Chem B. 7 (2019) 4811–4820. 10.1039/c9tb01028a. [PubMed: 31389966]

[15]. Casella A, Panitch A, Leach JK, Endogenous electric signaling as a blueprint for conductive materials in tissue engineering, Bioelectricity. (2020). 10.1089/bioe.2020.0027.

[16]. Zhao G, Feng Y, Xue L, Cui M, Zhang Q, Xu F, Peng N, Jiang Z, Gao D, Zhang X, Anisotropic conductive reduced graphene oxide/silk matrices promote post-infarction myocardial function by restoring electrical integrity, Acta Biomater. 139 (2022) 190–203. 10.1016/j.actbio.2021.03.073. [PubMed: 33836222]

[17]. Eftekhari BS, Eskandari M, Janmey PA, Samadikuchaksaraei A, Gholipourmalekabadi M, Surface topography and electrical signaling: single and synergistic effects on neural differentiation of stem cells, Adv Funct Mater. (2020) 1907792. 10.1002/adfm.201907792.

[18]. Engler AJ, Sen S, Sweeney HL, Discher DE, Matrix elasticity directs stem cell lineage specification, Cell. 126 (2006) 677–89. 10.1016/j.cell.2006.06.044. [PubMed: 16923388]

[19]. Branco da Cunha C, Klumpers DD, Li WA, Koshy ST, Weaver JC, Chaudhuri O, Granja PL, Mooney DJ, Influence of the stiffness of three-dimensional alginate/collagen-I interpenetrating networks on fibroblast biology, Biomaterials. 35 (2014) 8927–8936. 10.1016/J.BIOMATERIALS.2014.06.047. [PubMed: 25047628]

[20]. Chaudhuri O, Gu L, Klumpers D, Darnell M, Bencherif SA, Weaver JC, Huebsch N, Lee H-P, Lippens E, Duda GN, Mooney DJ, Hydrogels with tunable stress relaxation regulate stem cell fate and activity, Nat. Mater 15 (2016) 326–334. 10.1038/nmat4489. [PubMed: 26618884]

[21]. Leach JK, Whitehead J, Materials-directed differentiation of mesenchymal stem cells for tissue engineering and regeneration, ACS Biomater. Sci. Eng 4 (2018) 1115–1127. 10.1021/acsbiomaterials.6b00741. [PubMed: 30035212]

[22]. Falagan-Lotsch P, Grzincic EM, Murphy CJ, One low-dose exposure of gold nanoparticles induces long-term changes in human cells, Proc Natl Acad Sci. 113 (2016) 13318–13323. 10.1073/pnas.1616400113. [PubMed: 27821760]

[23]. Prajapati SK, Malaiya A, Kesharwani P, Soni D, Jain A, Biomedical applications and toxicities of carbon nanotubes, Drug Chem Toxicol. (2020) 1–16. 10.1080/01480545.2019.1709492.

[24]. Humpolicek P, Kasparkova V, Pachernik J, Stejskal J, Bober P, Capakova Z, Radaszkiewicz KA, Junkar I, Lehocky M, The biocompatibility of polyaniline and polypyrrole: A comparative study of their cytotoxicity, embryotoxicity and impurity profile, Mater Sci Eng C Mater Biol Appl. 91 (2018) 303–310. 10.1016/j.msec.2018.05.037. [PubMed: 30033259]

[25]. Mawad D, Mansfield C, Lauto A, Perbellini F, Nelson GW, Tonkin J, Bello SO, Carrad DJ, Micolich AP, Mahat MM, Furman J, Payne D, Lyon AR, Gooding JJ, Harding SE, Terracciano CM, Stevens MM, A conducting polymer with enhanced electronic stability applied in cardiac models, Sci Adv. 2 (2016) e1601007. 10.1126/sciadv.1601007. [PubMed: 28138526]

[26]. Spencer AR, Shirzaei Sani E, Soucy JR, Corbet CC, Primbetova A, Koppes RA, Annabi N, Bioprinting of a cell-laden conductive hydrogel composite, ACS Appl Mater Interfaces. 11 (2019) 30518–30533. 10.1021/acsami.9b07353. [PubMed: 31373791]

[27]. Zhang S, Chen Y, Liu H, Wang Z, Ling H, Wang C, Ni J, Celebi-Saltik B, Wang X, Meng X, Kim HJ, Baidya A, Ahadian S, Ashammakhi N, Dokmeci MR, Travas-Sejdic J, Khademhosseini A, Room-temperature-formed PEDOT:PSS hydrogels enable injectable, soft, and healable organic bioelectronics, Adv Mater. 32 (2020) e1904752. 10.1002/adma.201904752. [PubMed: 31657081]

[28]. Campbell KT, Stilhano RS, Silva EA, Enzymatically degradable alginate hydrogel systems to deliver endothelial progenitor cells for potential revasculature applications, Biomaterials. 179 (2018) 109–121. 10.1016/j.biomaterials.2018.06.038. [PubMed: 29980073]

[29]. Laurent TC, Determination of the structure of agarose gels by gel chromatography, Biochim. Biophys. Acta BBA - Gen. Subj 136 (1967) 199–205. 10.1016/0304-4165(67)90064-5.

[30]. Pluen A, Netti PA, Jain RK, Berk DA, Diffusion of Macromolecules in Agarose Gels: Comparison of Linear and Globular Configurations, Biophys. J 77 (1999) 542–552. 10.1016/S0006-3495(99)76911-0. [PubMed: 10388779]

[31]. Ho SS, Keown AT, Addison B, Leach JK, Cell migration and bone formation from mesenchymal stem cell spheroids in alginate hydrogels are regulated by adhesive ligand density, Biomacromolecules. 18 (2017) 4331–4340. 10.1021/acs.biomac.7b01366. [PubMed: 29131587]

[32]. Rechendorff K, Hovgaard MB, Foss M, Zhdanov VP, Besenbacher F, Enhancement of Protein Adsorption Induced by Surface Roughness, Langmuir. 22 (2006) 10885–10888. 10.1021/la0621923. [PubMed: 17154557]

[33]. Yixue S, Bin C, Yuan G, Chaoxi W, Lingmin Z, Peng C, Xiaoying W, Shunqing T, Modification of agarose with carboxylation and grafting dopamine for promotion of its cell-adhesiveness, Carbohydr. Polym 92 (2013) 2245–2251. 10.1016/j.carbpol.2012.12.003. [PubMed: 23399284]

[34]. Cambria E, Brunner S, Heusser S, Fisch P, Hitzl W, Ferguson SJ, Wuertz-Kozak K, Cell-laden agarose-collagen composite hydrogels for mechanotransduction studies, Front. Bioeng. Biotechnol 8 (2020). https://www.frontiersin.org/articles/10.3389/fbioe.2020.00346 (accessed October 6, 2022).

[35]. Spearman BS, Hodge AJ, Porter JL, Hardy JG, Davis ZD, Xu T, Zhang X, Schmidt CE, Hamilton MC, Lipke EA, Conductive interpenetrating networks of polypyrrole and polycaprolactone encourage electrophysiological development of cardiac cells, Acta Biomater. 28 (2015) 109–120. 10.1016/j.actbio.2015.09.025. [PubMed: 26407651]

[36]. Chen M-C, Sun Y-C, Chen Y-H, Electrically conductive nanofibers with highly oriented structures and their potential application in skeletal muscle tissue engineering, Acta Biomater. 9 (2013) 5562–72. 10.1016/j.actbio.2012.10.024. [PubMed: 23099301]

[37]. Malvankar NS, Vargas M, Nevin KP, Franks AE, Leang C, Kim BC, Inoue K, Mester T, Covalla SF, Johnson JP, Rotello VM, Tuominen MT, Lovley DR, Tunable metallic-like conductivity in microbial nanowire networks, Nat Nanotechnol. 6 (2011) 573–9. 10.1038/nnano.2011.119. [PubMed: 21822253]

[38]. Walimbe T, Calve S, Panitch A, Sivasankar MP, Incorporation of types I and III collagen in tunable hyaluronan hydrogels for vocal fold tissue engineering, Acta Biomater. 87 (2019) 97–107. 10.1016/j.actbio.2019.01.058. [PubMed: 30708064]

[39]. Vorwald CE, Gonzalez-Fernandez T, Joshee S, Sikorski P, Leach JK, Tunable fibrin-alginate interpenetrating network hydrogels to support cell spreading and network formation, Acta Biomater. 108 (2020) 142–152. 10.1016/j.actbio.2020.03.014. [PubMed: 32173582]

[40]. Song F, Jie W, Zhang T, Li W, Jiang Y, Wan L, Liu W, Li X, Liu B, Room-temperature fabrication of a three-dimensional reduced-graphene oxide/polypyrrole/hydroxyapatite composite scaffold for bone tissue engineering, RSC Adv. 6 (2016) 92804–92812. 10.1039/C6RA15267H.

[41]. Yang S, Jang Lindyk., Kim S, Yang J, Yang K, Cho S-W, Lee JY, Polypyrrole/alginate hybrid hydrogels: electrically conductive and soft biomaterials for human mesenchymal stem cell culture and potential neural tissue engineering applications, Macromol. Biosci 16 (2016) 1653–1661. 10.1002/mabi.201600148. [PubMed: 27455895]

[42]. Wu Y, Wang L, Guo B, Ma PX, Interwoven aligned conductive nanofiber yarn/hydrogel composite scaffolds for engineered 3D cardiac anisotropy, ACS Nano. 11 (2017) 5646–5659. 10.1021/acsnano.7b01062. [PubMed: 28590127]

[43]. Wang S, Guan S, Zhu Z, Li W, Liu T, Ma X, Hyaluronic acid doped-poly(3,4-ethylenedioxythiophene)/chitosan/gelatin (PEDOT-HA/Cs/Gel) porous conductive scaffold for nerve regeneration, Mater Sci Eng C Mater Biol Appl. 71 (2017) 308–316. 10.1016/j.msec.2016.10.029. [PubMed: 27987712]

[44]. Marzocchi M, Gualandi I, Calienni M, Zironi I, Scavetta E, Castellani G, Fraboni B, Physical and electrochemical properties of PEDOT:PSS as a tool for controlling cell growth, ACS Appl Mater Interfaces. 7 (2015) 17993–8003. 10.1021/acsami.5b04768. [PubMed: 26208175]

[45]. Funk RH, Monsees T, Ozkucur N, Electromagnetic effects - from cell biology to medicine, Prog Histochem Cytochem. 43 (2009) 177–264. 10.1016/j.proghi.2008.07.001. [PubMed: 19167986]

[46]. Kotwal A, Schmidt CE, Electrical stimulation alters protein adsorption and nerve cell interactions with electrically conducting biomaterials, Biomaterials. 22 (2001) 1055–64. 10.1016/s0142-9612(00)00344-6. [PubMed: 11352099]

[47]. Schmidt CE, Shastri VR, Vacanti JP, Langer R, Stimulation of neurite outgrowth using an electrically conducting polymer, Proc Nati Acad Sci USA. 94 (1997) 8948–53. 10.1073/pnas.94.17.8948.

[48]. Guo H, Uehara Y, Matsuda T, Kiyama R, Li L, Ahmed J, Katsuyama Y, Nonoyama T, Kurokawa T, Surface charge dominated protein absorption on hydrogels, Soft Matter. 16 (2020) 1897–1907. 10.1039/c9sm01999e. [PubMed: 31995092]

[49]. Pasche S, Voros J, Griesser HJ, Spencer ND, Textor M, Effects of ionic strength and surface charge on protein adsorption at PEGylated surfaces, J Phys Chem B. 109 (2005) 17545–52. 10.1021/jp050431+. [PubMed: 16853244]

[50]. Hartvig RA, Van De Weert M, Østergaard J, Jorgensen L, Jensen H, Protein Adsorption at Charged Surfaces: The Role of Electrostatic Interactions and Interfacial Charge Regulation, Langmuir. 27 (2011) 2634–2643. 10.1021/la104720n. [PubMed: 21322572]

[51]. Albertsson P-Å, Partition of Cell Particles and Macromolecules in Polymer Two-Phase Systems, in: Anfinsen CB, Edsall JT, Richards FM (Eds.), Adv. Protein Chem, Academic Press, 1970: pp. 309–341. 10.1016/S0065-3233(08)60244-2.

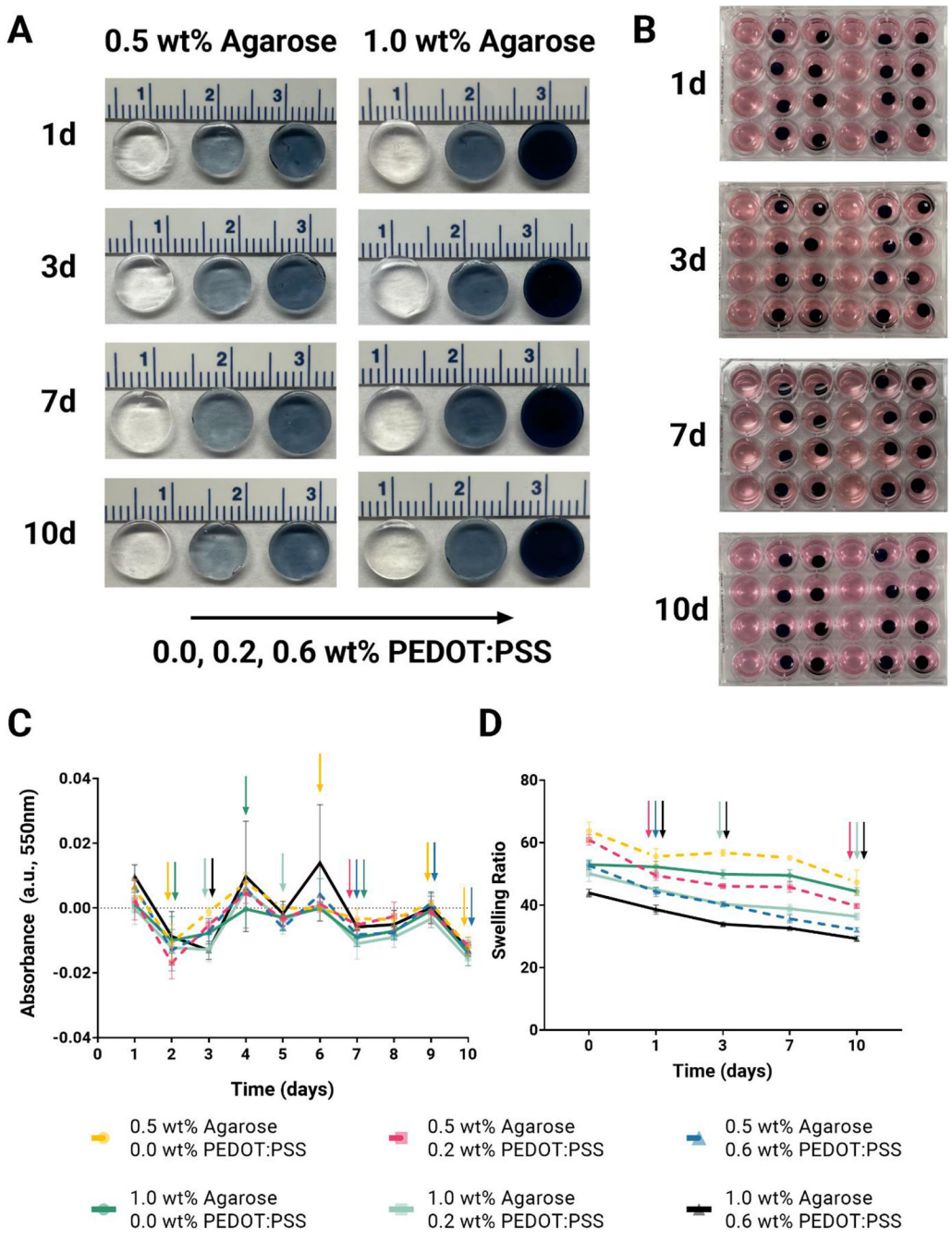

Figure 1: Hydrogels stored in αMEM maintain gross structure over 10 days.

(A) Gross images of agarose hydrogels with tunable mechanical ([agarose]) and electrical ([PEDOT:PSS]) properties over time. **(B)** Representative images illustrate the lack of color change of gel storage αMEM over time, indicating gel structural integrity. **(C)** Absorbance of hydrogel storage αMEM fluctuated over time but is not appreciably different than baseline. Arrows indicate a significant difference ($p \leq 0.05$) in absorbance between the marked timepoint and the one preceding it. **(D)** Hydrogel swelling ratio decreased steadily over time. Arrows indicate a significant difference ($p \leq 0.05$) in swelling ratio between the marked timepoint and the one preceding it.

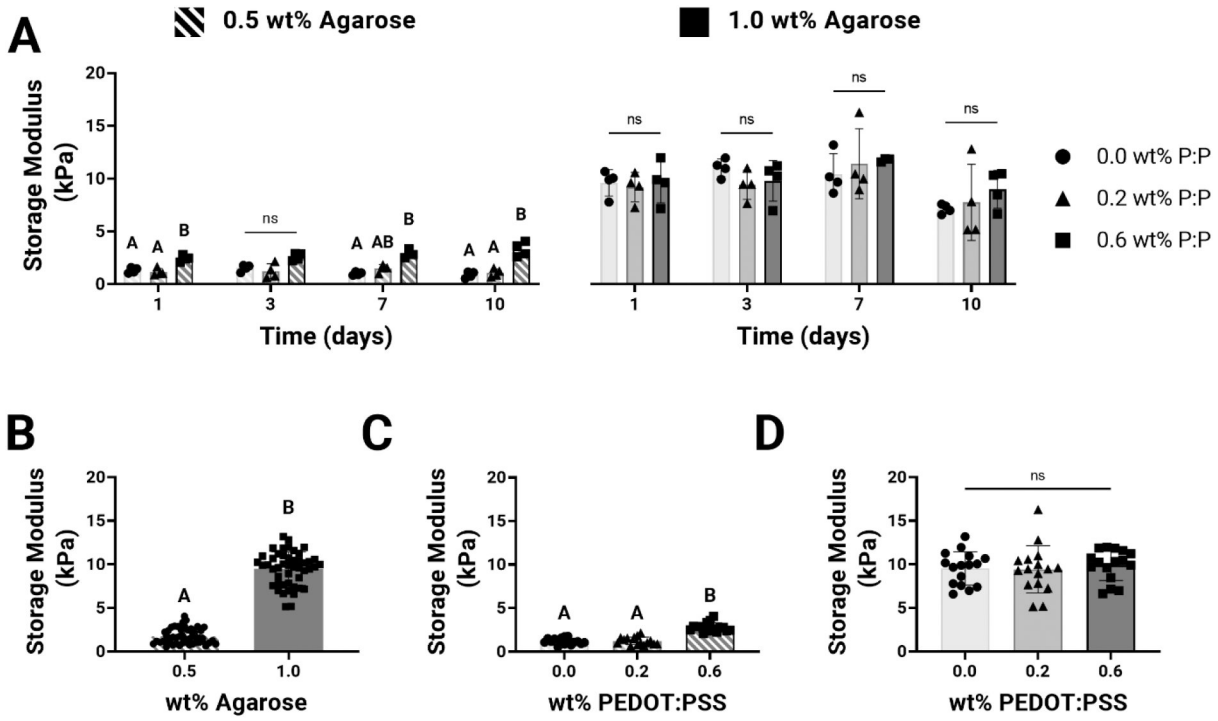

Figure 2: Storage modulus of hydrogels stored in αMEM is driven by agarose content.

(A) Mechanical properties were predominantly affected by wt% agarose, but addition of 0.6 wt% PEDOT:PSS caused significant increases in storage modulus of the 0.5 wt% agarose gels at most time points ($p \leq 0.05$ at 1 and 10d, $p \leq 0.01$ at 7d; n=3-4). Two-way ANOVA for the simple effect of PEDOT:PSS concentration was used to analyze the differences between groups within each timepoint. Tests were run separately for 0.5 and 1.0 wt% agarose gels. **(B)** Storage moduli of PEDOT:PSS-loaded agarose hydrogels was driven by wt% agarose ($p \leq 0.0001$; n=47-48), calculated with a two-tailed t-test. **(C)** Storage moduli of 0.5 wt% agarose gels increased with addition of 0.6 wt% PEDOT:PSS ($p \leq 0.0001$; n=16). **(D)** The storage moduli of 1.0 wt% agarose gels were unchanged by the addition of PEDOT:PSS ($p \leq 0.0001$; n=16). One-way ANOVA was used to analyze differences between groups for **(C)** and **(D)**. Groups denoted by different letters are statistically significant, ns=not significant.

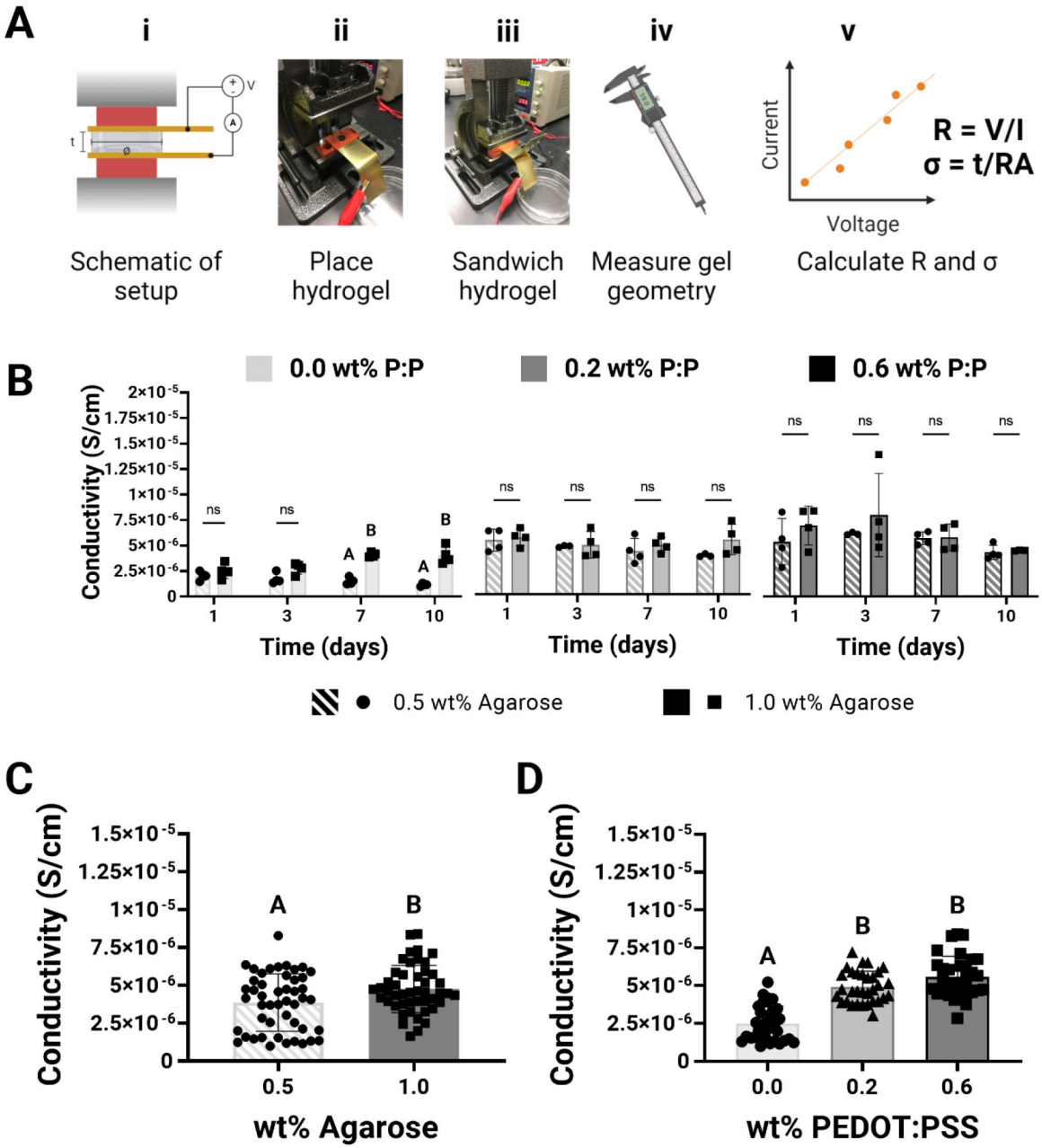

Figure 3: Hydrogel conductivity is driven by PEDOT:PSS concentration.

(A) i: Schematic of conductivity setup, where ii) hydrogels are placed on one brass plate and contained by a PDMS sheet. The hydrogel is then iii) sandwiched between both brass plates. The power supply connected to one plate provides a source of voltage and a multimeter connected to the other plate displays output current. After taking current measurements, (iv) hydrogel geometric parameters are recorded and (v) current-voltage curves are generated. I-V curves are assessed for linearity and used to calculate resistance. **(B)** Conductivity is predominantly driven by wt% PEDOT:PSS. Differences in the conductivity of 0.5 and 1.0 wt% agarose groups containing no PEDOT:PSS indicate some intrinsic conductivity of agarose ($p \leq 0.01$; n=3-4). The differences due to agarose concentration were not

observed in PEDOT:PSS-containing groups. Multiple t-tests for the simple effect of agarose concentration were used to analyze the differences between groups within each timepoint. Tests were run separately for the 0.0, 0.2, and 0.6 wt% PEDOT:PSS gels. **(C)** Pooled data eliminating the contribution of wt% PEDOT:PSS indicate conductivity of gels increases with increasing agarose content ($p \leq 0.05$; n=47-48), calculated with a two-tailed t-test. **(D)** When conductivity is analyzed as a function of wt% PEDOT:PSS, the level of significance is much greater ($p \leq 0.0001$; n=31-32). One-way ANOVA was used to analyze differences between groups. Groups denoted by different letters are statistically significant; ns=not significant.

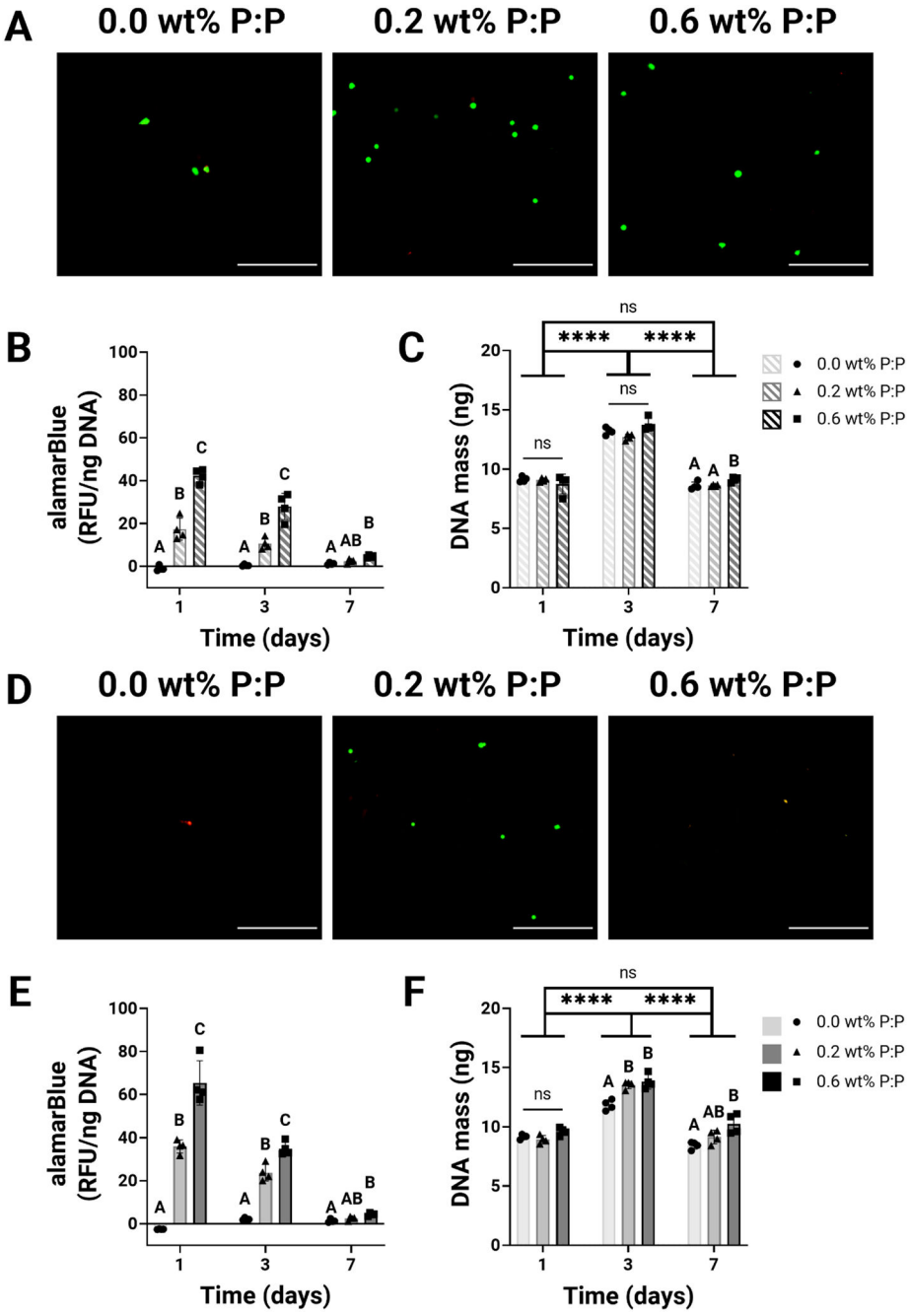

Figure 4: Conductivity supports cell viability and metabolic activity of MSCs at early timepoints.

(A) LIVE/DEAD images of MSCs on 0.5 wt% agarose gels indicate overall viability of adhered cells at 7d. Gels containing at least 0.2 wt% PEDOT:PSS supported greater cell adhesion compared to non-conductive controls (10X objective, scale bars = 500 μm). **(B)** Metabolic activity of cells cultured on 0.5 wt% agarose gels was significantly greater when the substrate was conductive ($p \leq 0.05$ for 3d, $p \leq 0.01$ for 1 and 7d; n=4). **(C)** DNA mass was nearly constant between groups within each timepoint ($p \leq 0.05$ for 7d) but was highest overall on 3d ($p \leq 0.0001$). **(D)** LIVE/DEAD staining of MSCs grown on 1.0 wt% agarose gels indicate similar cell behavior, though the 0.2 wt% PEDOT:PSS group supported cell

adhesion and viability better than the 0.6 wt% PEDOT:PSS group. **(E)** Metabolic activity of cells cultured on 1.0 wt% agarose gels was also greater when the gel was conductive ($p \leq 0.05$ for 1 and 7d, $p \leq 0.01$ for 3d; n=4). **(F)** DNA mass increased with PEDOT:PSS concentration on 3 and 7d ($p \leq 0.05$), but was highest overall on 3d ($p \leq 0.0001$). Two-way ANOVA for the simple effect of PEDOT:PSS concentration was used to determine differences between groups within each timepoint for **(B),(C),(E),** and **(F)**. Two-way ANOVA for the main effect of time was used to determine overall differences between timepoints for **(C)** and **(F)**. Groups denoted by different letters are statistically significant within each time point, ns=not significant.

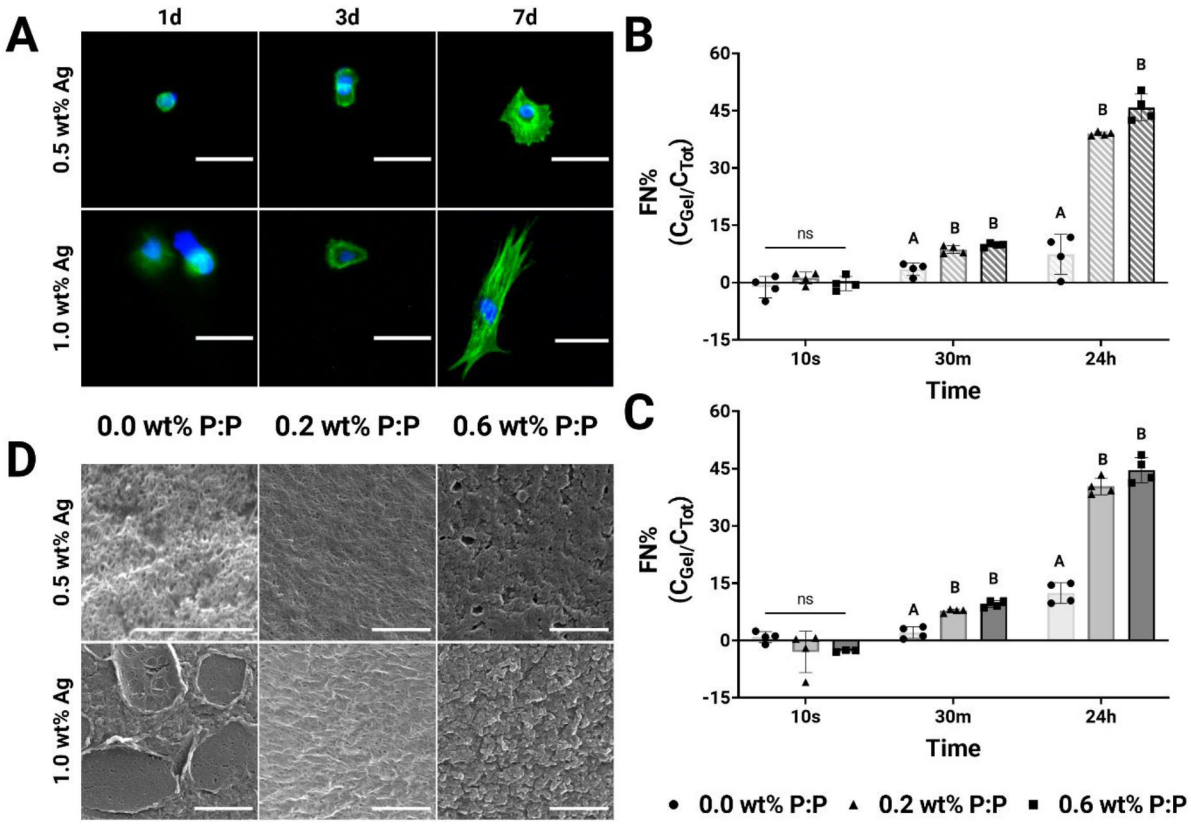

Figure 5: Conductive hydrogels support greater cell adhesion and spreading even in the absence of binding sites.

(A) Cells adhered to and spread more effectively on conductive substrates compared to non-conductive controls. Cell cytoskeleton was stained for phalloidin (green), and nuclei were stained with DAPI (blue) (10X objective, scale bars = 50 μm). **(B)** The concentration of adsorbed fibronectin (FN) to 0.5 wt% agarose gels increased with increasing concentrations of PEDOT:PSS ($p \leq 0.05$ for 30 min, $p \leq 0.01$ for 24 h; n=4). **(C)** Similarly, FN adsorbed better to conductive 1.0 wt% agarose gels ($p \leq 0.05$ for 30 min, $p \leq 0.01$ for 24 h; n=4). **(D)** Scanning electron micrographs of hydrogels demonstrate surface network characteristics (50,000X objective for 0.5 wt% Ag. + 0.0 wt% P:P; 25,000X objective for all other groups; scale bars = 1 μm). Two-way ANOVA for the simple effect of PEDOT:PSS concentration was used to analyze the differences between groups within each timepoint for **(B)** and **(C)**. Groups denoted by different letters are statistically significant, ns=not significant.

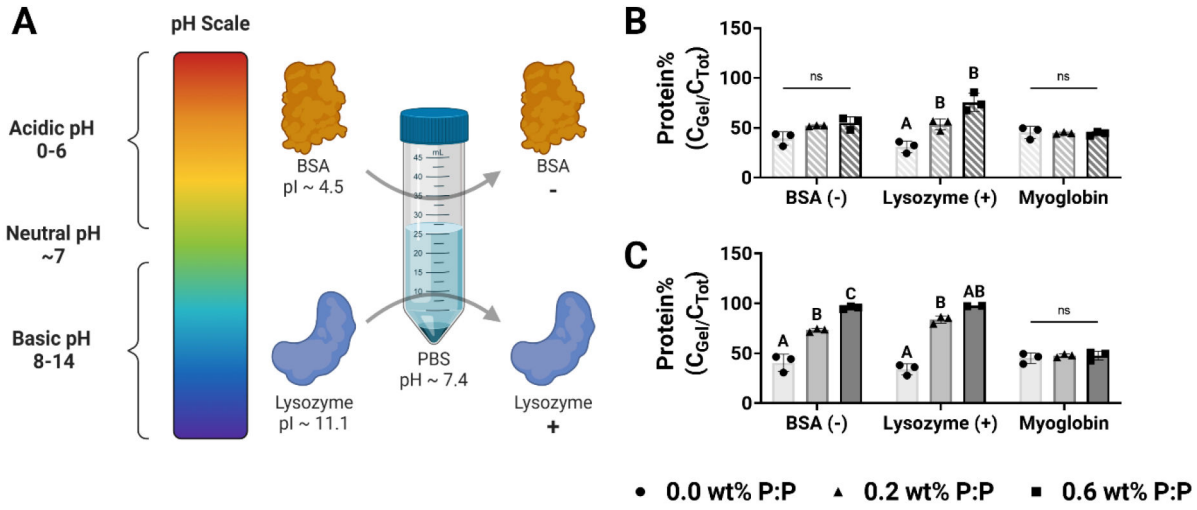

Figure 6: Conductivity facilitates the adsorption of charged proteins.

(A) Schematic illustrating proteins with different isoelectric points become charged when dissolved in a neutral solvent. **(B)** Conductive 0.5 wt% agarose gels facilitate greater adsorption of the positively charged protein, lysozyme, compared to the non-conductive control ($p \leq 0.05$). Further, adsorption of the neutral protein, myoglobin, is unaffected by substrate conductivity (n=3). **(C)** Similar behavior is observed with 1.0 wt% agarose gels, though differences were observed for both charged proteins ($p \leq 0.05$; n=2-3). Two-way ANOVA for the simple effect of PEDOT:PSS concentration was used to analyze the differences between groups within each protein solution. Groups denoted by different letters are statistically significant within each protein group, ns=not significant.

Table 1:

Mechanically and electrically tunable hydrogel formulations

Final wt% agarose	Final wt% PEDOT:PSS	Volume of 2.5 wt% agarose (μL)	Volume of 1.0 wt% PEDOT:PSS (μL)	Volume of water (μL)
0.5	0.0	100	0.0	400
	0.2		100	300
	0.6		300	100
1.0	0.0	200	0.0	300
	0.2		100	200
	0.6		300	0